Clinical Ophthalmology

Dovepress
Taylor & Francis Group

Open Access Full Text Article

ORIGINAL RESEARCH

Structural Characteristics of Parapapillary Choroidal Microvasculature Dropout in Primary Open-Angle Glaucoma: Comparison Between Width and Area

Seung Hyen Lee[1], Jeong Hyun Seo[1], Geun Young Moon[1], Alex S Huang[2], Tae-Woo Kim[3], Eun Ji Lee[3]

[1]Department of Ophthalmology, Nowon Eulji Medical Center, Eulji University College of Medicine, Seoul, Korea; [2]Hamilton Glaucoma Center, The Viterbi Family Department of Ophthalmology, Shiley Eye Institute, University of California, San Diego, CA, USA; [3]Department of Ophthalmology, Seoul National University College of Medicine, Seoul National University Bundang Hospital, Seongnam, Korea

Correspondence: Seung Hyen Lee, Department of Ophthalmology, Nowon Eulji Medical Center, Eulji University College of Medicine, 68 Hangulbiseok-ro, Nowon-gu, Seoul, 01830, Korea, Tel +82 2 970 8000, Fax +82 2 970 8429, Email dramyle83@gmail.com

Purpose: To compare the circumferential width and area of parapapillary choroidal microvasculature dropout (CMvD) and investigate their correlation with clinical characteristics in eyes with primary open-angle glaucoma (POAG).

Subjects and methods: This retrospective cross-sectional study included 121 POAG eyes with localized retinal nerve fiber layer (RNFL) defects (84 eyes with CMvD and 37 without CMvD). CMvD was defined as focal sectoral capillary hypoperfusion or nonperfusion in the parapapillary choroid identified using optical coherence tomography angiography. Circumferential CMvD width (in degrees) and area were quantitatively measured, and their relationships with clinical factors were analyzed.

Results: CMvD was present in 84 of 121 eyes (69.4%). Although CMvD width and area were strongly correlated ($P<0.001$), they showed distinct clinical associations. A larger CMvD width was significantly associated with a thinner global RNFL thickness ($P=0.046$), worse visual field mean deviation ($P=0.049$), and larger β-zone parapapillary atrophy (PPA) area ($P=0.013$). Conversely, larger areas of β-zone and γ-zone PPA were related to a larger CMvD area ($P=0.001$ and $P<0.001$, respectively).

Conclusion: Although circumferential CMvD width and area were highly correlated, their associated clinical factors differed. The CMvD width, reflecting the extent of optic disc margin involvement, serves as a more robust indicator of glaucomatous damage severity than the CMvD area, which may be influenced more by myopia-related anatomical variation.

Keywords: primary open-angle glaucoma, choroidal microvasculature dropout, optical coherence tomography angiography, ocular blood flow

Introduction

Recent advancements in imaging modalities, particularly optical coherence tomography angiography (OCTA), have provided new insights into the role of vascular factors in the pathogenesis and progression of glaucoma.[1–4] OCTA enables non-invasive, high-resolution visualization of the choroidal microvasculature, and numerous studies have demonstrated that parapapillary choroidal microvasculature dropout (CMvD) is strongly associated with glaucomatous damage.[5–8] Specifically, its localization and presence have been closely linked to the site of neuroretinal rim thinning and corresponding visual field (VF) defects.[9,10]

Longitudinal studies have suggested that changes in CMvD size are linked to glaucoma progression, implying that the morphological characteristics of CMvD may carry additional clinical significance.[11–13] However, the specific quantitative descriptors of CMvD that most accurately reflect the severity of hemodynamic compromise remain poorly understood. Although both circumferential width and area have been used to quantify CMvD, it is unclear whether these metrics represent distinct structural properties or have clinical implications.

https://doi.org/10.2147/OPTH.S614845
Received: 6 April 2026
Accepted: 23 May 2026
Published: 5 June 2026

We hypothesized that the circumferential width of the CMvD along the optic disc margin and its area represent different structural properties and would show distinct clinical associations in eyes with primary open-angle glaucoma (POAG). Therefore, we aimed to compare CMvD width and area and investigate their correlation with glaucomatous structural and functional parameters.

Methods

Study Design and Subjects

This retrospective cross-sectional study included consecutive patients who visited the Glaucoma Clinic at Nowon Eulji University Hospital between April 2022 and July 2024. This study was approved by the Institutional Review Board of Nowon Eulji University Hospital (no. 2022–09-024), which waived the requirement for informed consent due to the retrospective nature of the study. Conducted in adherence to the tenets of the Declaration of Helsinki, the study ensured that all patient data were anonymized and maintained with strict confidentiality.

All participants underwent a comprehensive ophthalmic examination, including a detailed medical history of hypertension and diabetes mellitus, best-corrected visual acuity assessment, slit-lamp biomicroscopy, Goldmann applanation tonometry, refraction, gonioscopy, and dilated stereoscopic fundus examination. Color and red-free fundus photography (TRC-NW8; Topcon, Tokyo, Japan), central corneal thickness (CCT) and axial length (AXL) measurements (Lenstar LS900, Haag-Streit, Koeniz, Switzerland), standard automated perimetry (24–2 Swedish interactive threshold algorithm and Humphrey automated field analyzer III 860, Humphrey Instruments, Carl Zeiss, CA, USA), circumpapillary RNFL thickness, and scanning of the optic disc using spectral-domain OCT (SD-OCT) and OCT angiography (OCTA, Spectralis, Heidelberg Engineering, Heidelberg, Germany) were also performed.

Eligible subjects were required to have primary open-angle glaucoma (POAG) with a single focal RNFL defect that was clearly visible on infrared fundus imaging and to undergo OCTA imaging. The exclusion criteria were as follows: (1) diffuse or multiple RNFL defects that could interfere with accurate CMvD measurements. (2) History of ocular surgery other than uncomplicated cataract or glaucoma surgery, coexisting intraocular diseases other than glaucoma (eg, diabetic retinopathy or non-glaucomatous optic neuropathy), or neurologic diseases (eg, stroke or pituitary tumor) that could confuse visual field (VF) results. (3) Unreliable VF tests or poor-quality images of OCT/OCTA images. When both eyes met the inclusion criteria, only one eye was randomly selected.

POAG was defined as the presence of an open iridocorneal angle, signs of glaucomatous optic nerve damage (ie., neuroretinal rim thinning, notching, or RNFL defect), or a corresponding glaucomatous VF defect. Glaucomatous VF damage was defined as (1) values outside the normal limits on a glaucoma hemifield test, (2) three abnormal points with $< 5\%$ probability of being normal, one with $< 1\%$ by pattern deviation, or (3) pattern standard deviation (PSD) outside 95% normal limits as confirmed on two consecutive, reliable tests. VFs were considered reliable if the fixation losses were less than 20% and the false-positive and false-negative response rates were less than 25%.

Untreated intraocular pressure (IOP) was defined as the mean of at least two measured IOP before the initiation of ocular hypotensive treatment, and scan IOP was defined as the measured IOP at the time of OCTA imaging.

OCTA Imaging and Assessment of Circumferential Width and Area of CMvD

The optic nerve head and parapapillary regions were imaged using a Spectralis OCTA module (Heidelberg Engineering, Heidelberg, Germany). This system operates at a central wavelength of 880 nm with an acquisition speed of 85 kHz, providing lateral and axial resolutions of 5.7 μm and 3.9 μm per pixel, respectively. Scans were obtained using a $10° \times 10°$ scan pattern consisting of 512 clusters of five repeated B-scans centered on the optic disc. Spectralis OCTA uses a full-spectrum probabilistic approach that computes the probability that a given pixel represents perfused vasculature rather than static tissue. This algorithmic approach produces high-contrast, nearly binary images of the microvascular network by effectively distinguishing flow signals from background noise.[14]

CMvD was defined as a focal, sectoral dropout of the parapapillary choroidal microvasculature with no visible microvascular network on deep-layer en-face OCTA images.[1,5,15] The en-face OCTA image was aligned with the same orientation as the infrared fundus image from the Spectralis OCT system by superimposing the OCTA image over the IR

image using Photoshop (version 12.0; Adobe Systems, Figure 1a). The CMvD width on the choroidal slab was measured using ImageJ software (version 1.51; National Institutes of Health, Bethesda, Maryland, USA). Two lines were drawn connecting the disc center to the circumferential margin of the CMvD, and the angle between these two lines was defined as the MvD width in degrees (Figure 1b). The CMvD area was manually delineated using the tool provided by the Spectralis OCT viewer software (Heidelberg Eye Explorer software version 1.7.0.0; Heidelberg Engineering), corrected for the magnification by the optic media of the eye, and expressed in millimeters squared. Areas covered by large retinal vessels were included in the CMvD when the dropout extended beyond the vessels; otherwise, vessel areas were excluded (Figure 1c). Two observers (J.H.S. and S.H.L.) who were blinded to the clinical characteristics of the participants independently assessed the presence, width, and area of the CMvD. Interobserver agreement and reproducibility were evaluated to minimize potential observer bias. Photoshop was used solely for topographic alignment between OCTA and infrared fundus images to ensure accurate anatomical correspondence. The mean CMvD width and area measured by the 2 observers were used for the analysis. Disagreements between observers regarding the presence and location of CMvD were resolved by a third adjudicator (T-W. K.).

Parapapillary Atrophy (PPA) and Juxtapapillary Choroidal Thickness (JPCT)

Parapapillary atrophy (PPA) was identified and quantified using infrared fundus and B-scan images provided by Spectralis OCT (Heidelberg Eye Explorer software version 1.7.0.0; Heidelberg Engineering). PPA was classified into two types according to the presence or absence of Bruch's membrane (BM), and the area was measured separately. β-zone PPA was defined as an atrophic area with intact BM between the termination of BM and the beginning of the retinal pigment epithelium (RPE).[16,17] γ-zone PPA was defined as an area of exposed scleral flange devoid of a BM–RPE complex or choroidal tissue (Figure 1d and e).[17,18] Two experienced masked observers (J.H.S. and S.H.L.) independently demarcated the borders on cross-sectional B-scans and measured the areas (mm^2) on infrared images. Each observer performed two measurements, and the mean of the four measurements was used for analysis.

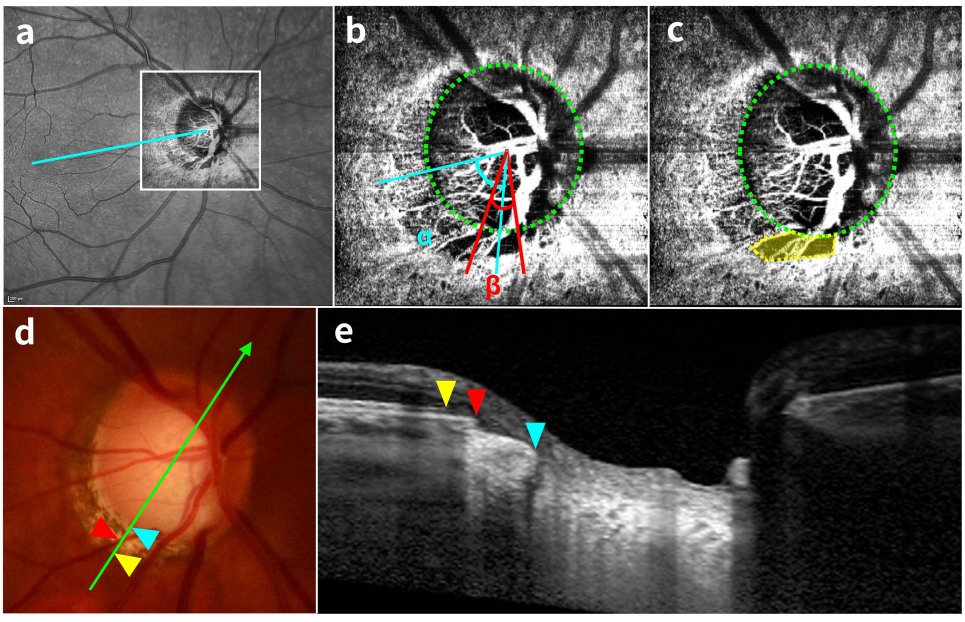

Figure 1 Measurement of parapapillary microvasculature dropout (CMvD), parapapillary atrophy (PPA), and juxtapapillary choroidal thickness (JPCT). (**a**) The en-face OCTA image is superimposed onto the Infrared fundus image to ensure topographic alignment. The *cyan line* represents the fovea-optic disc center axis, which serves as the reference. (**b** and **c**) Deep layer en-face OCTA images with the green dotted lines indicating the optic disc margin. The *cyan lines* indicates the angular location of the CMvD center relative to the fovea-disc axis (α). The *red lines* indicate the angle between them defines the circumferential width (β). The CMD area is manually delineated (*yellow shaded area*), The *green arrow* in fundus photograph (**d**) indicates corresponding cross-sectional B-scan in (**e**). The *red arrowhead* indicates the optic disc margin. The *yellow arrowhead* points to the temporal edge of the Bruch's membrane, and the *cyan arrowhead* denotes the point where the sclera is exposed. The distances between these points define the β-zone and γ-zone PPA, respectively.

https://doi.org/10.2147/OPTH.S614845

Juxtapapillary choroidal thickness (JPCT) was defined as the vertical distance from the BM to the choroid-sclera interface in the juxtapapillary region. As previously described, the choroidal area within 500 μm from the border tissue of Elschnig was measured on a central horizontal B-scan and the JPCT was calculated by dividing the measured choroidal area by 500 μm.[19]

Statistical Analysis

Interobserver agreement for CMvD presence was assessed using kappa statistics (κ value), and interobserver reproducibility of CMvD width and area, PPA area, and JPCT was evaluated using the intraclass correlation coefficient (ICC). Continuous variables were compared using the Student's *t*-test, and categorical variables were compared using the chi-squared test. Multiple linear regression analyses were performed to investigate factors associated with CMvD width and area. First, univariable linear regression was conducted for each potential predictor, and variables with $P<0.1$ were then entered into the multivariable linear regression model. To assess potential multicollinearity among correlated factors variance inflation factors (VIFs) were calculated for all multivariable models. No substantial multicollinearity was observed (all VIFs<2). Statistical analyses were performed using SPSS software (version 22.0; SPSS, Chicago, IL, USA), and $P<0.05$.

Result

Characteristics of Study Subjects

In total, 137 eyes initially met the inclusion criteria. Of these eyes, 16 were excluded because of poor-quality OCTA images, and the remaining 121 eyes were included in the final analysis. Among these, CMvD was observed in 84 eyes (69.4%) at the location of the localized RNFL defect. Interobserver agreement for the presence of CMvD was excellent (κ=0.995). The interobserver reliability for quantifying CMvD width and area demonstrated high reproducibility, with ICCs of 0.978 and 0.953, respectively.

The demographic and ocular characteristics of the participants are summarized in Table 1. Compared with eyes without CMvD, the group with CMvD had a higher proportion of females ($P=0.028$), worse visual field results ($P<0.001$), thinner global RNFL thickness ($P<0.001$), and larger β-PPA area ($P=0.004$).

Table 1 Characteristics of Subjects

Variables	Eyes without CMvD (n=37)	Eyes with CMvD (n=84)	*P* value
Age, years	62.5 ± 9.6	63.8 ± 13.0	0.545
Male / Female	23 / 14	34 / 50	**0.028**
Diabetes mellitus (n, %)	12 (32.4)	18 (21.4)	0.197
Hypertension (n, %)	17 (45.9)	29 (34.5)	0.233
Axial length, mm	24.16 ± 1.22	24.06 ± 1.37	0.729
Central corneal thickness, μm	537.1 ± 25.3	528.0 ± 29.5	0.375
Untreated IOP, mmHg	15.7 ± 2.7	16.5 ± 3.1	0.255
Scan IOP, mmHg	13.1 ± 2.1	12.6 ± 2.5	0.361
VF MD, dB	−1.83 ± 2.60	−6.40 ± 5.12	**<0.001**
VF PSD, dB	3.74 ± 2.77	8.92 ± 4.49	**<0.001**
Global RNFL thickness, μm	83.1 ± 6.9	73.3 ± 12.1	**<0.001**
CMvD width, °	n/a	37.95 ± 21.88	n/a
CMvD area, mm^2	n/a	0.15 ± 0.14	n/a
Beta PPA area, mm^2	0.59 ± 0.45	0.90 ± 0.56	**0.004**
Gamma PPA area, mm^2	0.07 ± 0.18	0.15 ± 0.29	0.065

Notes: Values area mean± standard deviation unless otherwise indicated. Values with statistical significance (*P*<0.05) are shown in bold.

Abbreviations: CMvD, choroidal microvascular dropout; IOP, intraocular pressure; VF, visual field; MD, mean deviation; PSD, pattern standard deviation; RNFL, retinal nerve fiber layer; n/a, not applicable; PPA, parapapillary atrophy.

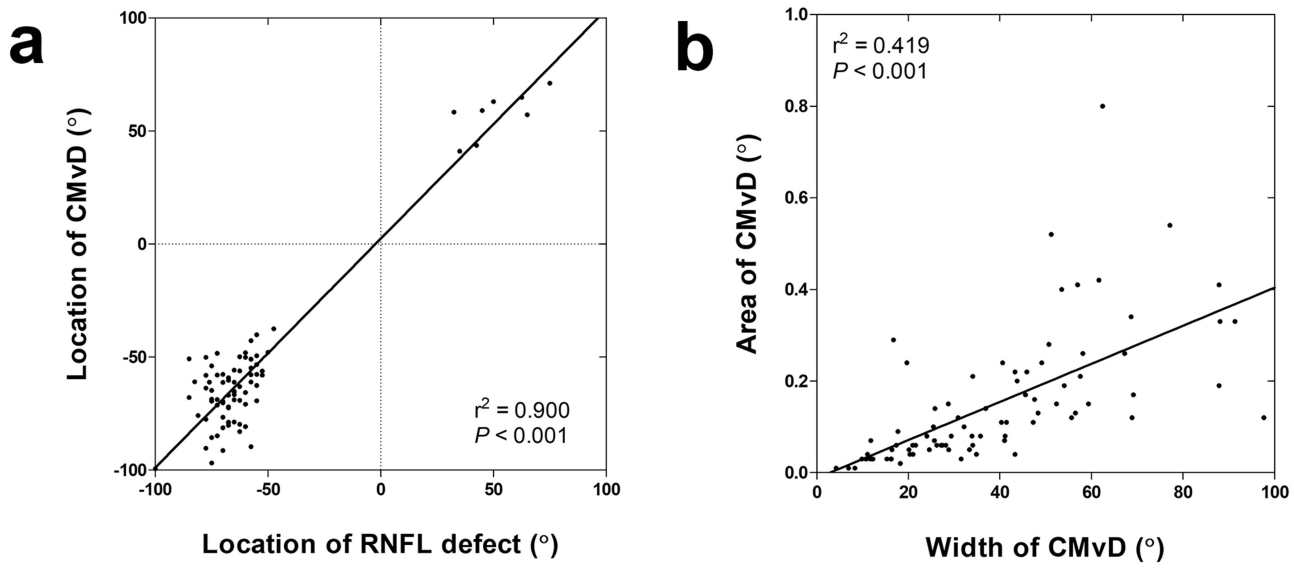

Figure 2 Topographic and morphologic correlation of parapapillary CMvD. (**a**) Scatterplot illustrating a strong positive correlation between the angular location of the CMvD and localized RNFL defect. (**b**) Scatterplot showing the correlation between the circumferential width and the area of the CMvD.

Topographic Correspondence and Morphological Characteristics of CMvD

Among the 84 eyes (69.4%) identified with CMvD, the angular location of each dropout was topographically coincident with the site of the localized RNFL defect in all cases (r^2=0.900, P<0.001, Figure 2a) The circumferential width and area of CMvD were significantly correlated (r^2=0.419, P<0.001, Figure 2b). The mean CMvD width was 37.95±21.88°, and the mean area was 0.15±0.14 mm^2.

Factors Associated with CMvD Width and Area

Univariate and multivariate linear regression analyses of factors associated with CMvD width and area are presented in Table 2. In the multivariable model, an increased circumferential width of the CMvD was significantly associated with a worse VF mean deviation (P=0.046), thinner global RNFL thickness (P=0.049), and larger β-PPA area (P=0.013, Figure 3a–c).

Table 2 Factors Associated with the Width and Area of MvD in Eyes with MvD (n=84)

Variables	Width of CMvD					Area of CMvD				
	Univariable		Multivariable Analysis			Univariable		Multivariable Analysis		
	Beta	*P*	Beta	*P*	VIF	Beta	*P*	Beta	*P*	VIF
Age, years	0.481	**0.009**	0.226	0.261	1.343	0.002	0.072	0.002	0.072	1.542
Gender	3.118	0.525				0.007	0.836			
Diabetes	5.417	0.355				0.002	0.951			
Hypertension	1.501	0.767				−0.025	0.444			
Axial length, mm	−0.622	0.725				0.009	0.429			
Central corneal thickness, μm	0.013	0.878				0.001	0.917			
Untreated IOP, mmHg	−0.185	0.815				−0.005	0.280			
Scan IOP, mmHg	−0.954	0.330				−0.008	0.189			
VF MD, dB	−1.584	**0.001**	−0.965	**0.046**	1.342	−0.005	0.114			
Global RNFL thickness, μm	−0.731	**<0.001**	−0.411	**0.049**	1.412	−0.003	**0.015**	−0.002	0.137	1.077
JPCT, μm	−204.052	0.075	−109.705	0.321	1.199	−2.050	**0.005**	−0.992	0.156	1.199
Beta PPA area, mm^2	13.251	**0.002**	9.951	**0.013**	1.067	0.093	**0.001**	0.094	**0.001**	1.286
Gamma PPA area, mm^2	−5.170	0.539				0.104	0.052	0.201	**<0.001**	1.288

Notes: Variables with P<0.1 in the univariable analysis were included in the multivariable analysis. Values with statistical significance (P<0.05) are shown in bold.
Abbreviations: CMvD, choroidal microvascular dropout; VIF, variance inflation factor; IOP, intraocular pressure; VF, visual field; MD, mean deviation; RNFL, retinal nerve fiber layer; JPCT, juxtapapillary choroidal thickness; PPA, parapapillary atrophy.

https://doi.org/10.2147/OPTH.S614845

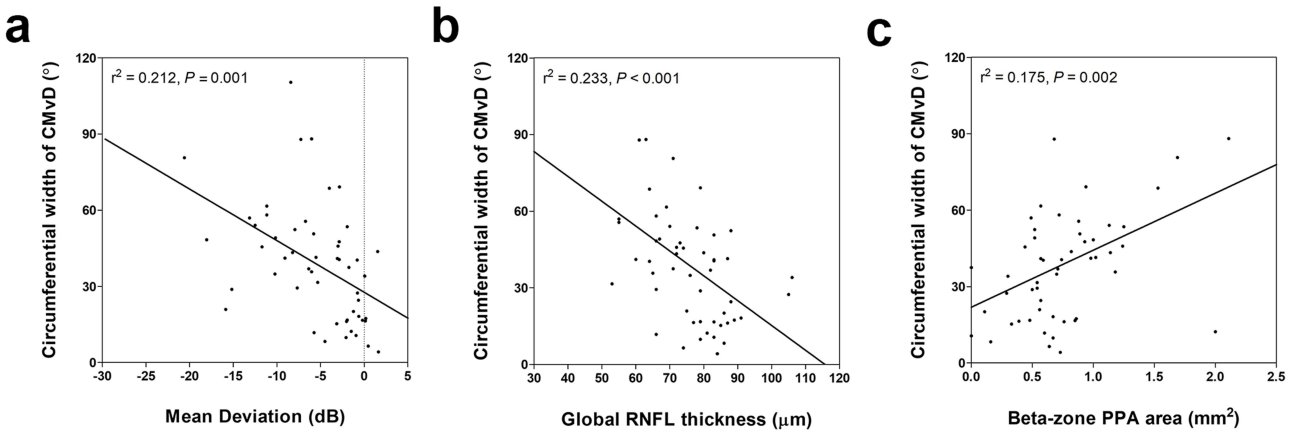

Figure 3 Association between circumferential CMvD width and clinical factors. Scatterplot showing a significant linear association between the CMvD width and (**a**) visual field mean deviation, (**b**) global RNFL thickness, and (**c**) β-zone PPA area. It should be noted that an increase in CMvD width was significantly associated with the clinical parameters related to glaucoma severity.

In contrast, a larger CMvD area was significantly associated only with a larger area of β-PPA and γ-PPA (P=0.001 and P<0.001, respectively), whereas other functional and structural glaucomatous parameters did not reach statistical significance.

Representative Cases

Figure 4 and 5 show two POAG eyes with localized RNFL defects. The eye in Figure 4 shows a relatively advanced glaucomatous damage despite relatively small CMvD area. The circumferential CMvD width at the disc margin relatively wide (Figure 4a), whereas the manually delineated CMvD area (Figure 4b) appears small. Correspondingly, structural and functional glaucomatous damage are advanced on the RNFL thickness map (Figure 4c) and visual field defect (Figure 4d). It can be seen that the deep structure of the optic disc has only β-zone PPA (Figure 4e and f). On the other

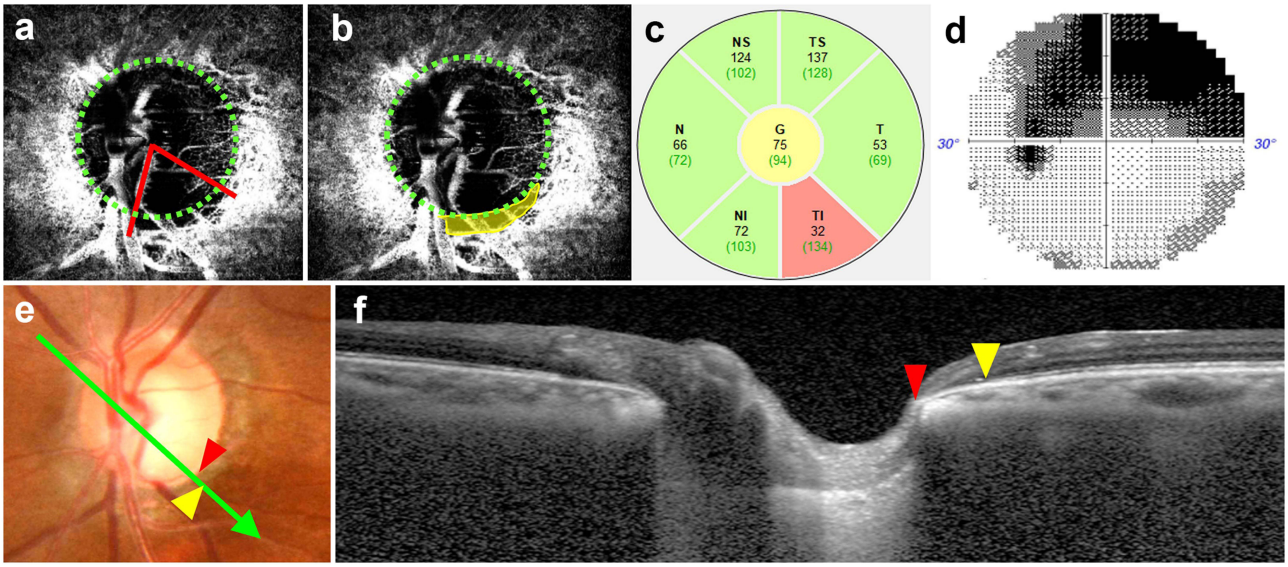

Figure 4 Representative case of a wide circumferential CMvD. An 82-year-old female presented with prominent circumferential CMvD width. (**a** and **b**) Deep-layer en-face OCTA images with *green dotted lines* indicating the optic disc margin. (**a**) *red lines* delineate the circumferential margins of the CMvD corresponding to the CMvD width at the disc margin. (**b**) The *yellow shaded area* represents the manually delineated CMvD area, which appears relatively limited compared to the wide width. (**c**) Global RNFL thickness map and (**d**) visual field test reveals glaucomatous damage. In the fundus photograph (**e**), the *green arrow* indicates the location and direction of the cross-sectional OCT B-scan (**f**). The distance between the *red arrowhead* (Bruch's membrane opening) and *yellow arrowhead* (edge of the retinal pigment epithelium) represents the width of the β-zone PPA. A significantly wide CMvD, even with a relatively limited area, is associated with substantial functional and structural glaucomatous damage.

https://doi.org/10.2147/OPTH.S614845

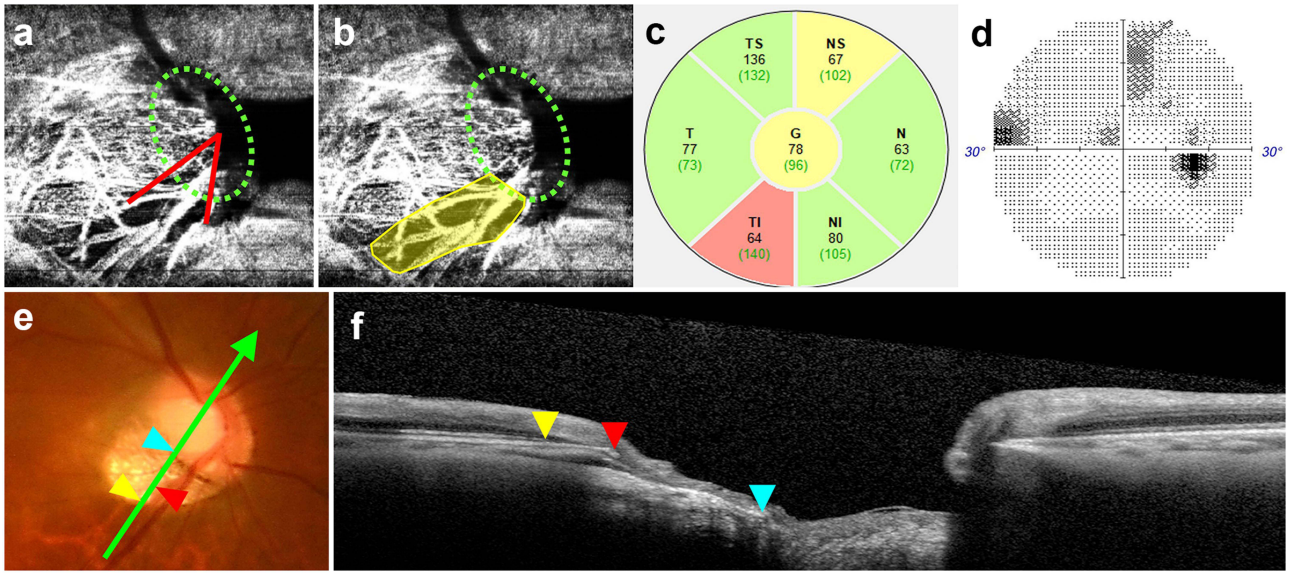

Figure 5 Representative case of a narrow CMvD width with a large area. A 55-year-old male presented with CMvD with an extensive area but a narrow width. (a and b) Deep-layer en-face OCTA images with *green dotted lines* indicating the optic disc margin. (**a**) *red lines* delineate the circumferential margins of the CMvD corresponding to the CMvD width at the disc margin. (**b**) The *yellow shaded area* represents the manually delineated CMvD area, which appears extensively large compared to the narrow width. (**c**) Global RNFL thickness map and (**d**) visual field test reveals mild glaucomatous damage. In the fundus photograph (**e**), the *green arrow* indicates the location and direction of the cross-sectional OCT B-scan (**f**). The *red, yellow, and cyan arrowheads* indicate the optic disc margin, the temporal edge of the Bruch's membrane, and the exposed sclera, respectively. The distances between these points define the β-zone (*red to yellow*) and γ-zone (*red to cyan*) PPA, which is relatively larger than that of the β-zone PPA. Note that An extensively large CMvD area may not necessarily reflect severe glaucomatous damage, if the circumferential CMvD width at the disc margin remains narrow.

hand, the eye with a relatively narrow width of CMvD (Figure 5a), but a wide area of CMvD (Figure 5b) shows relatively early glaucomatous damage (Figure 5c and d). The optic disc was tilted and had a wider γ-zone PPA than β-zone PPA (Figure 5e and f).

Discussion

This study demonstrated that CMvD was present in approximately 70% of POAG eyes with a localized RNFL defect, and was associated with worse VF damage, thinner RNFL, and larger β-zone PPA. Quantitative assessment of both the circumferential width and area of the CMvD showed that the circumferential width of the CMvD had a stronger correlation with structural and functional glaucomatous damage than the CMvD area. These findings suggest that the extent of optic disc margin involvement, as quantified by CMvD width, more be more closely associated with the vascular compromise in glaucoma than CMvD area.

The optic nerve head is primarily supplied by two distinct arterial systems. The short posterior ciliary artery (SPCA) circulates to the peripapillary choroid, prelaminar tissue, and lamina cribrosa mainly through the circle of Zinn-Haller, a vascular ring around the ONH. The central retinal artery (CRA) supplies the inner retinal layers and superficial optic nerve head region.[20,21] CMvD detected by OCTA reflects sectoral capillary loss within the SPCA circulation territory, thus signifying localized vascular insufficiency of the prelaminar and laminar optic nerve head tissues that are most vulnerable to glaucomatous injury.[4,22] Our results show a precise topographic coincidence[11,12] between CMvD and RNFL defects (Figure 2), reinforcing the pathogenic link between SPCA-derived vascular impairment and glaucomatous axonal loss.[5,6]

Although the width and area were strongly correlated, this study highlights a subtle but clinically meaningful distinction between these two metrics. Previous longitudinal studies have demonstrated that an increase in the "size" of CMvD is associated with glaucoma progression. However, the specific parameters used to quantify this size vary in literature. For instance, some researchers have focused on the CMvD area to represent the total extent of vascular loss, whereas others have utilized circumferential width as a primary indicator.

https://doi.org/10.2147/OPTH.S614845

This lack of standardized measurements has led to ambiguity regarding the metric that captures glaucomatous damage more effectively. Our multivariable analysis addresses this by showing that CMvD width has a significantly stronger correlation with VF mean deviation and RNFL thickness than CMvD area. Since the width specifically reflects the extent of involvement at the optic disc margin, a crucial vascular interface where SPCA-derived microvessels converge, it may be more closely associated with the disruption of blood supply to the prelaminar and laminar tissues than to the total radial area.[23]

Interestingly, CMvD width was only associated with β-zone PPA, whereas CMvD area was correlated with both β- and γ-zone PPA. Since γ-zone PPA typically results from myopia-related scleral stretching and Bruch's membrane displacement,[18] the association of the CMvD area with the γ-zone suggests that it may partially reflect biomechanical alterations rather than purely glaucomatous vascular dropout.[15,16,24] This further supports the use of the width as a more specific surrogate for glaucomatous damage.

This study had several limitations that should be considered. First, its cross-sectional design precludes causal interference with the extent of the CMvD and glaucomatous progression. Second, only eyes with a single localized RNFL defect were included, which may limit the generalizability of the findings. However, this criterion was applied to ensure a clear topographic association between CMvD and glaucomatous damage. Another limitation of this study is the lack of a dedicated myopic eye group. Therefore, the relationship between CMvD and myopia should be interpreted with caution. Additionally, the sample size may limit generalizability across all glaucoma phenotypes. However, the high interobserver agreement and reliability of the CMvD measurements strengthened the validity of our comparative analysis.

In conclusion, despite the strong correlation between CMvD width and area, CMvD width is closely associated with glaucomatous damage. CMvD width may be associated with glaucomatous damage by capturing the critical involvement of the optic disc margin.

Data Sharing Statement

The datasets generated and/or analyzed during the current study are available from the corresponding author upon reasonable request.

Acknowledgment

This paper was previously presented at the ARVO 2024 as a poster presentation with interim findings. The corresponding abstract was published in "Poster Abstracts" in ARVO Annual Meeting abstract: June 2024, Volume 65, Issue 7.

https://iovs.arvojournals.org/article.aspx?articleid=2794869.

Funding

This work was supported by an Eulji Research Grant (EJRG-25-05) funded by Eulji University in 2025.

Disclosure

The authors declare that they have no conflicts of interest in this work.

References

1. Suh MH, Zangwill LM, Manalastas PI, et al. Deep retinal layer microvasculature dropout detected by the optical coherence tomography angiography in glaucoma. *Ophthalmology*. 2016;123(12):2509–2518. doi:10.1016/j.ophtha.2016.09.002
2. Jia Y, Wei E, Wang X, et al. Optical coherence tomography angiography of optic disc perfusion in glaucoma. *Ophthalmology*. 2014;121(7):1322–1332. doi:10.1016/j.ophtha.2014.01.021
3. Jia Y, Morrison JC, Tokayer J, et al. Quantitative OCT angiography of optic nerve head blood flow. *Biomed Opt Express*. 2012;3(12):3127–3137. doi:10.1364/boe.3.003127
4. Flammer J, Orgul S, Costa VP, et al. The impact of ocular blood flow in glaucoma. *Prog Retin Eye Res*. 2002;21(4):359–393. doi:10.1016/s1350-9462(02)00008-3
5. Lee EJ, Lee KM, Lee SH, Kim TW. Parapapillary choroidal microvasculature dropout in glaucoma: a comparison between optical coherence tomography angiography and indocyanine green angiography. *Ophthalmology*. 2017;124(8):1209–1217. doi:10.1016/j.ophtha.2017.03.039
6. Lee EJ, Lee SH, Kim JA, Kim TW. Parapapillary deep-layer microvasculature dropout in glaucoma: topographic association with glaucomatous damage. *Invest Ophthalmol Vis Sci*. 2017;58(7):3004–3010. doi:10.1167/iovs.17-21918

7. Kashani AH, Chen C-L, Gahm JK, et al. Optical coherence tomography angiography: a comprehensive review of current methods and clinical applications. *Prog Retin Eye Res*. 2017;60:66–100. doi:10.1016/j.preteyeres.2017.07.002
8. Spaide RF, Fujimoto JG, Waheed NK, Sadda SR, Staurenghi G. Optical coherence tomography angiography. *Prog Retin Eye Res*. 2018;64:1–55. doi:10.1016/j.preteyeres.2017.11.003
9. Lee EJ, Lee KM, Lee SH, Kim TW. OCT angiography of the peripapillary retina in primary open-angle glaucoma. *Invest Ophthalmol Vis Sci*. 2016;57(14):6265–6270. doi:10.1167/iovs.16-20287
10. Lee EJ, Kim J-A, Kim T-W. Influence of choroidal microvasculature dropout on the rate of glaucomatous progression: a prospective study. *Ophthalmol Glaucoma*. 2020;3(1):25–31. doi:10.1016/j.ogla.2019.10.001
11. Lee JY, Shin JW, Song MK, Hong JW, Kook MS. An increased choroidal microvasculature dropout size is associated with progressive visual field loss in open-angle glaucoma. *Am J Ophthalmol*. 2021;223:205–219. doi:10.1016/j.ajo.2020.10.018
12. Kim J-A, Lee EJ, Kim T-W. Evaluation of parapapillary choroidal microvasculature dropout and progressive retinal nerve fiber layer thinning in patients with glaucoma. *JAMA Ophthalmol*. 2019;137(7):810–816. doi:10.1001/jamaophthalmol.2019.1212
13. Shoji T, Zangwill LM, Akagi T, et al. Progressive macula vessel density loss in primary open-angle glaucoma: a longitudinal study. *Am J Ophthalmol*. 2017;182:107–117. doi:10.1016/j.ajo.2017.07.011
14. Rocholz R, Teussink MM, Dolz-Marco R, et al. SPECTRALIS optical coherence tomography angiography (OCTA): principles and clinical applications. *Heidelb Eng Acad*. 2018;1.
15. Lee EJ, Kim TW, Lee SH, Kim JA. Underlying microstructure of parapapillary deep-layer capillary dropout identified by optical coherence tomography angiography. *Invest Ophthalmol Vis Sci*. 2017;58(3):1621–1627. doi:10.1167/iovs.17-21440
16. Kim M, Kim TW, Weinreb RN, Lee EJ. Differentiation of parapapillary atrophy using spectral-domain optical coherence tomography. *Ophthalmology*. 2013;120(9):1790–1797. doi:10.1016/j.ophtha.2013.02.011
17. Dai Y, Jonas JB, Huang H, Wang M, Sun X. Microstructure of parapapillary atrophy: beta zone and gamma zone. *Invest Ophthalmol Vis Sci*. 2013;54(3):2013–2018. doi:10.1167/iovs.12-11255
18. Jonas JB, Jonas SB, Jonas RA, et al. Parapapillary atrophy: histological gamma zone and delta zone. *PLoS One*. 2012;7(10):e47237. doi:10.1371/journal.pone.0047237
19. Lee SH, Lee EJ, Kim TW. Topographic correlation between juxtapapillary choroidal thickness and parapapillary deep-layer microvasculature dropout in primary open-angle glaucoma. *Br J Ophthalmol*. 2018;102(8):1134–1140. doi:10.1136/bjophthalmol-2017-311136
20. Hayreh SS. Blood supply of the optic nerve head and its role in optic atrophy, glaucoma, and oedema of the optic disc. *Br J Ophthalmol*. 1969;53(11):721–748. doi:10.1136/bjo.53.11.721
21. Hayreh SS. Blood flow in the optic nerve head and factors that may influence it. *Prog Retin Eye Res*. 2001;20(5):595–624. doi:10.1016/s1350-9462(01)00005-2
22. Weinreb RN, Khaw PT. Primary open-angle glaucoma. *Lancet*. 2004;363(9422):1711–1720. doi:10.1016/s0140-6736(04)16257-0
23. Burgoyne CF, Downs JC, Bellezza AJ, Suh JK, Hart RT. The optic nerve head as a biomechanical structure: a new paradigm for understanding the role of IOP-related stress and strain in the pathophysiology of glaucomatous optic nerve head damage. *Prog Retin Eye Res*. 2005;24(1):39–73. doi:10.1016/j.preteyeres.2004.06.001
24. Lee EJ, Kim TW, Kim JA, Kim JA. Parapapillary deep-layer microvasculature dropout in primary open-angle glaucoma eyes with a parapapillary gamma-zone. *Invest Ophthalmol Vis Sci*. 2017;58(13):5673–5680. doi:10.1167/iovs.17-22604